



MINISTRY OF SUPPLY

AERONAUTICAL RESEARCH COUNCIL  
REPORTS AND MEMORANDA

A Theoretical Investigation into the Lateral  
Stability of an Aeroplane Controlled by an  
Automatic Pilot, with Particular Reference to  
the Effect of Flight Path Angle

By

T. W. PRESCOTT, M.ENG.

*Crown Copyright Reserved*

LONDON: HER MAJESTY'S STATIONERY OFFICE

1952

THREE SHILLINGS NET

# A Theoretical Investigation into the Lateral Stability of an Aeroplane Controlled by an Automatic Pilot, with Particular Reference to the Effect of Flight Path Angle

By

T. W. PRESCOTT, M.ENG.

COMMUNICATED BY THE PRINCIPAL DIRECTOR OF SCIENTIFIC RESEARCH (AIR),  
MINISTRY OF SUPPLY

*Reports and Memoranda No. 2640*

*January, 1948\**

*Summary.*—Several autopilots produce aileron deflection proportional to the movement between the aeroplane and the outer gimbal of a vertical gyroscope. In non-level flight this relative movement is not equal to the rotation of the aeroplane about its  $x$ -axis, and it was desirable to investigate the lateral stability for steep angles of climb and dive.

Calculations show that instability does occur, but that stability can be restored either by making the rudder deflection dependent on aileron movement in order to counteract the aileron drag coefficient, or by adding a rate of yaw term to the rudder circuit. The addition of both aileron and rate terms to the rudder circuit is greatly superior to the addition of either term alone.

The aileron drag coefficient can also have a detrimental effect at the start of an automatic turn, and response curves during entry into the turn have been calculated for various degrees of aileron drag compensation. The bank angle and sideslip response curves are unaffected by the compensation. The rate of turn response is improved during the first second but subsequently is little affected by aileron drag compensation.

1. *Introduction.*—1.1. In an automatic pilot using a vertical axis gyroscope for defining the vertical it is customary to move the ailerons proportional to the angle between the aeroplane and the outer gimbal ring. In level flight this will give the conventional system of aileron applied being proportional to the bank angle of the aeroplane.

In non-level flight, however, the deflection of the outer gimbal is  $\{\phi + \tan^{-1}(\tan \gamma_e \sin \psi)\}$  where

$\phi$  is rotation of aeroplane about its  $x$ -axis,

$\psi$  is rotation of aeroplane about its  $z$ -axis,

$\gamma_e$  is the aeroplane's angle of climb.

Provided that  $\psi$  and  $\psi \tan \gamma_e$  are small the outer gimbal deflection is approximately  $(\phi + \psi \tan \gamma_e)$ , and so the aileron equation becomes

$$\begin{aligned} \xi &= F(\phi + \psi \tan \gamma_e) \\ &= F_\phi \phi + F_\psi \psi. \end{aligned} \quad \dots \dots \dots (1)$$

The rudder equation considered is of the form

$$\zeta = H_\psi \psi, \quad \dots \dots \dots (2)$$

where

$\xi$  is amount of aileron applied,

$\zeta$  is amount of rudder applied,

$F, H_\psi$ , are autopilot parameters.

\* R.A.E. Technical Note I.A.P. 974—received 15th April, 1948.

It is known that a roll control of the form

$$\xi = F_\phi \phi + F_\psi \psi \quad \dots \quad (3)$$

produces an unstable oscillation as  $F_\psi$  is increased positively. This instability is mainly due to the aileron drag coefficient, and it was desired to know at what angle of climb instability occurred. Making  $F_\psi$  increasingly negative in equation (3) results in a subsidence becoming negatively damped, and so instability was also feared in a dive ( $\tan \gamma_e$  is negative).

In this report methods of stabilizing the aeroplane's motion are considered, including aileron drag compensation, and the addition of a rate of yaw term to the rudder equation.

1.2. The effect of the aileron drag coefficient at the start of an automatic turn has been investigated using the lateral control equations for an autopilot now under development. Level flight has been assumed as this autopilot also suffers from the defect mentioned in section 1.1. Exact compensation and over compensation of  $\mathcal{N}_\xi$ , the aileron drag coefficient, have been tried in an attempt to improve the entry into an automatic turn, and the results are included in this report.

2. *Lateral Stability in Climb and Dive.*—In the calculations the aerodynamic derivatives used are those of a Meteor jet fighter flying at 600 m.p.h. at sea level. Variation of the derivatives proportional to the lift coefficient  $C_L$ , ( $k$ ,  $k_1$ ,  $n_1$ , and  $l_2$ ) with angles of climb and dive has been neglected, as stability boundary calculations showed it to have very little effect on the stability of the system. Similarly, changing the climbing speed to 300 m.p.h. at sea level also had little effect on stability.

2.1. *Conventional Displacement Control.*—The control equations considered,

$$\xi = 2(\phi + \psi \tan \gamma_e),$$

and

$$\zeta = 4\psi,$$

give a fifth order stability equation when combined with the non-dimensional form of the lateral equations of motion of the aeroplane (4).

$$\left. \begin{aligned} \dot{\phi}' + \dot{\phi} \bar{y}_v + \psi' - k\phi - k_1\psi &= 0 \\ \phi'' + l_1\phi' - l_2\psi' + \mathcal{L}\dot{\phi} + \mathcal{L}_\xi\xi &= 0 \\ \psi'' + n_2\psi' + n_1\phi' - \mathcal{N}\dot{\phi} + \mathcal{N}_\zeta\zeta - \mathcal{N}_\xi\xi &= 0 \end{aligned} \right\} \dots \dots (4)$$

In equation (4), dashes denote differentiation with respect to  $\tau$ , the time measured in airsecs (one airsec is  $\bar{l}$  true sec);  $\dot{\phi} = \dot{\psi}/U_e$ ; and the aerodynamic derivatives  $\bar{y}_v$ ,  $k$ ,  $l_1$ , etc. are defined by Mitchell<sup>1</sup>. The unit of aerodynamic time,  $\bar{l}$ , is given by the equation

$$\bar{l} = \frac{m}{\rho S U_e} \text{ true sec,}$$

where

$m$  is the mass of the aeroplane (slugs),

$S$  is the wing area (sq ft),

$U_e$  is the forward speed of the aeroplane (ft/sec),

$\rho$  is the air density (slugs/cu ft).

The fifth order stability discriminant yields a poorly damped subsidence, a well damped 'roll' oscillation, and a poorly damped 'yaw' oscillation. Thus for the level flight case the stability factors are

$$\begin{aligned} &(\lambda + 0.1639)(\lambda^2 + 6.4200\lambda + 112.3189)(\lambda^2 + 0.3991\lambda + 51.2717) \\ &= (\lambda + 0.1639)(\lambda + 3.2100 \pm 10.1002i)(\lambda + 0.1996 \pm 7.1576i) \end{aligned}$$

The damping factors are plotted in Fig. 1 for  $\gamma_e = 70, 0$ , and  $-70$  deg, and it can be seen that the yaw oscillation becomes unstable at an angle of climb of 27 deg. This instability at such a small angle of climb is mainly due to the aileron drag coefficient,  $\mathcal{N}_\xi$ .

2.2. *Addition of a Rate of Yaw Term to the Rudder Equation.*—The rudder equation was modified to

$$\zeta = 4\psi + 0.98\psi', \quad \dots \dots \dots \quad (5)$$

and the damping factors of the resulting motion plotted in Fig. 2 for  $\gamma_e = 70, 0$  and  $-70$  deg. The addition of the rate term  $0.98\psi'$  increases the total damping in the system by an amount  $0.98\mathcal{N}_\xi = 10.78$  ( $\mathcal{N}_\xi = 11$  for a Meteor flying at sea level), and it was expected that all this extra damping would appear on the yaw oscillation. In fact this happens when  $\gamma_e = 0$ , the stability factors being

$$(\lambda + 0.1639)(\lambda^2 + 6.4200\lambda + 112.3189) (\lambda^2 + 0.3991\lambda + 51.2717)$$

and

$$(\lambda + 0.1629)(\lambda^2 + 6.5193\lambda + 112.6298) (\lambda^2 + 11.0808\lambda + 51.4371),$$

without and with the rate term respectively. In a climb, however, the yaw oscillation also acquires some damping from the roll oscillation, whilst in a dive it loses some damping to the roll oscillation. The poorly damped subsidence is unaltered by either the change in  $\gamma_e$  or the addition of the rate term.

It may happen that the amount of rate term that can be injected into the rudder circuit is limited by physical considerations, and it is uncertain how much of it may be necessary to overcome the inherent phase lags in the system. Hence there may not be enough rate term available in the rudder equation to restore stability in a steep climb.

2.3. *Compensation for the Aileron Drag Coefficient.*—By moving the rudder an amount proportional to the aileron deflection it is possible to compensate for the aileron drag coefficient,  $\mathcal{N}_\xi$ , of the aeroplane. The rudder equation becomes

$$\zeta = 4\psi + H_\xi\xi, \quad \dots \dots \dots \quad (6)$$

where  $H_\xi$  is an autopilot parameter, exact compensation for  $\mathcal{N}_\xi$  being obtained when  $H_\xi \mathcal{N}_\xi = \mathcal{N}_\xi$ . For the Meteor flying at sea level,  $\mathcal{N}_\xi = 3$ , and therefore for exact compensation,  $H_\xi = 3/11 = 0.2727$ . The damping factors of the motion when  $H_\xi = 0.2727$  are plotted in Fig. 3 for  $\gamma_e$  from  $-70$  deg to  $+70$  deg. In level flight the damping factors are very nearly equal to those of the uncompensated case, but are practically unaltered by change in  $\gamma_e$ . However, the damping of the yaw oscillation decreases slightly as  $\gamma_e$  increases positively and the oscillation becomes unstable at a climb angle of  $87$  deg, a great improvement on the  $27$  deg climb angle of the uncompensated case. The instability is now mainly caused by the aerodynamic derivative  $n_p$  (the yawing moment due to rate of roll).

In Fig. 4,  $H_\xi = 0.5454$  (100 per cent over compensation for  $\mathcal{N}_\xi$ ), and the damping factors are plotted for  $\gamma_e = 70, 0$ , and  $-70$  deg. In the over-compensated case the yaw oscillation becomes unstable when the aeroplane is in a dive; but as  $\gamma_e$  increases positively, the yaw oscillation becomes better-damped at the expense of the roll oscillation. The subsidence is unaffected by change in either  $H_\xi$  or  $\gamma_e$ .

2.4. *Addition of Both Rate and Aileron Terms to the Rudder Equation.*—The rudder equation used was

$$\zeta = 4\psi + 0.98\psi' + H_\xi\xi. \quad \dots \dots \dots \quad (7)$$

The damping factors are plotted in Figs. 5 and 6 for  $H_\xi = 0.2727$  and  $0.5454$  respectively, with  $\gamma_e$  varied from  $-70$  deg to  $+70$  deg. Again, with exact compensation of the aileron drag coefficient, variation in  $\gamma_e$  has little effect on the stability of the motion. The extra damping added to the system by the rate term has all appeared on the yaw oscillation without affecting either the roll oscillation or the subsidence. Hence by combining exact aileron drag compensation with the addition of a rate of yaw term to the rudder equation it is possible to obtain the benefits of both sections 2.2 and 2.3. Over compensation of  $\mathcal{N}_\xi$  ( $H_\xi = 0.5454$ ) has the same destabilizing effect in dives as under compensation has in climbs.

3. *Automatic Turns Entry.*—The proposed lateral control equations of an autopilot are

$$\xi = 0.7905\phi' + 3\phi - 2\phi_D + 2.53 \int (\phi - \phi_D)d\tau, \quad \dots \dots \dots (8)$$

and

$$\zeta = 0.5\psi' - 1.0 \int \dot{\psi}d\tau + H_\xi \xi, \quad \dots \dots \dots (9)$$

where  $\phi_D$  is a constant under the control of the human pilot.  $\phi_D$  does not affect the stability of the system, and is zero in straight flight. If the pilot wishes to execute an automatic turn he changes  $\phi_D$  by moving a controller. This causes aileron to be applied in response to which the aeroplane will roll and finally execute a co-ordinated turn at a bank angle equal to  $\phi_D$ . Aileron and rudder to trim in the turn are supplied by the appropriate integral terms in equations (8) and (9).

If  $H_\xi = 0$  no rudder is applied at  $\tau = 0$ , the commencement of the turn. But since aileron is applied at  $\tau = 0$  the adverse yawing moment due to the aileron drag makes the aeroplane turn the wrong way. This causes the aeroplane to sideslip and rudder will be applied to make the aeroplane turn in the right direction. Hence with no compensation for  $\mathcal{N}_\xi$  the turns entry is not particularly smooth (see Fig. 7).

Response curves for  $\dot{\psi}$ ,  $\phi$ , and  $\psi'$ , using the above two control equations are plotted in Figs. 7, 8, and 9, respectively for  $H_\xi = 0, 0.2727$ , and  $0.5454$ . These values of  $H_\xi$  are equivalent to no compensation, exact compensation, and 100 per cent over compensation for  $\mathcal{N}_\xi$ . The aeroplane derivatives used in these calculations are for a Meteor flying at 110 m.p.h. at sea level with flaps and undercarriage down as it was considered that these derivatives would produce the worst turns entries.

On examination of Figs. 7, 8, and 9, it is seen that change in  $H_\xi$  has very little effect on the  $\phi$  and  $\dot{\psi}$  curves. At the larger values of  $H_\xi$  the initial  $\psi'$  motion is improved but after one second change in  $H_\xi$  has little effect even on the  $\psi'$  motion.

4. *Conclusions.*—(a) With no compensation for aileron drag the motion becomes unstable when the aeroplane is at a climb angle of greater than 27 deg. An unexpected result was the continued stability in a dive. This is probably due to the fact that an uncontrolled aeroplane is more stable in a dive than in level flight (Frayn and Parnell<sup>2</sup>).

(b) Whilst the addition of a rate of yaw term to the rudder circuit can restore stability, physical reasons may limit the amount which can be applied and insufficient may be available when the aeroplane is in a steep climb.

(c) With exact compensation for aileron drag the stability of the motion is uninfluenced by variation in climb and dive angle, but over compensation can lead to instability in a dive.

(d) Exact compensation for aileron drag and the addition of all the available rate of yaw term to the rudder circuit is the best combination to counteract instability in steep climbs and dives.

(e) Exact aileron drag compensation reduces the swing in the wrong direction but otherwise has little effect on the entry into an automatic turn; over compensation prevents the initial swing in the wrong direction experienced in the uncompensated case.

#### LIST OF SYMBOLS

<i>Symbol</i>	<i>Section defined</i>	<i>Meaning</i>
$b$	Appendix	Aeroplane wing span
$C_L$	2	Lift coefficient, $mg \cdot \cos \gamma_e / \frac{1}{2}\rho S U_e^2$
$\gamma_e$	1.1	Angle of climb in undisturbed flight

LIST OF SYMBOLS—continued

Symbol	Section defined	Meaning
$F, F_\phi, F_\psi$	1.1	Autopilot parameters
$\phi$	1.1	Angular displacement of aeroplane about $x$ -axis
$\phi_D$	3	Bank datum, desired bank angle
$g$	Appendix	Acceleration due to gravity
$H_\psi, H_\xi$	1.1, 2.3	Autopilot parameters
$i_A$	Appendix	Aeroplane inertia coefficient about $x$ -axis
$i_C$	Appendix	Aeroplane inertia coefficient about $z$ -axis
$k$	2.1	$\frac{1}{2}C_L$
$k_1$	2.1	$k \tan \gamma_e$
$l_1$	2.1	Rotary damping coefficient in roll — $l_p/i_A$
$l_2$	2.1	$l_r/i_A$
$l_p, l_r, l_u, l_\xi$	Appendix	Rolling moments due to rate of roll, rate of yaw, sideslip, and aileron angle
$\mathcal{L}$	2.1	— $\mu_2 l_u/i_A$
$\mathcal{L}_\xi$	2.1	Aileron rolling effect coefficient, — $\mu_2 l_\xi/i_A$
$m$	2.1	Mass of aeroplane
$\mu_2$	Appendix	Relative density of aeroplane. $2m/\rho S b$
$n_1$	2.1	— $n_p/i_C$
$n_2$	2.1	Rotary damping coefficient in yaw, — $n_r/i_C$
$n_p, n_r, n_u, n_\xi, n_\zeta$	Appendix	Yawing moments due to rate of roll, rate of yaw, sideslip, aileron angle, and rudder angle
$\mathcal{N}$	2.1	$\mu_2 n_u/i_C$
$\mathcal{N}_\xi$	1.2	Aileron yawing effect coefficient, $\mu_2 n_\xi/i_C$
$\mathcal{N}_\zeta$	2.1	Rudder yawing effect coefficient, — $\mu_2 n_\zeta/i_C$
$\psi$	1.1	Angular displacement of aeroplane about $z$ -axis
$\rho$	2.1	Air density
$S$	2.1	Aeroplane wing area
$t$	2.1	Unit of time in non-dimensional system, $m/\rho S U_e$
$\tau$	2.1	Time in airsecs
$U_e$	2.1	Forward speed in undisturbed flight
$v$	2.1	Component of speed along $y$ -axis (sideslip)
$\hat{v}$	2.1	Non-dimensional form of $v$ , $v/U_e$ (angle of sideslip)
$\xi$	1.1	Aileron movement from equilibrium position
$y_v$	Appendix	Non-dimensional form of force component along $y$ -axis due to sideslip
$\bar{y}_v$	2.1	— $y_v$
$\zeta$	1.1	Rudder movement from equilibrium position.

## REFERENCES

No.	Author	Title, etc.
1	K. Mitchell	A Supplementary Notation for Theoretical Lateral Stability Investigations. R.A.E. Tech. Note No. Aero. 1183 (Misc.). May, 1943. A.R.C. 6797. (Unpublished).
2	E. M. Frayn and M. V. Parnell	The Theoretical Effect of Flight Path Angle on the Lateral Stability and Response of an Aeroplane. R. & M. 2529. November, 1945.

## APPENDIX

*Data for Meteor type jet fighter flying at sea level*

$\frac{mg}{S} = 31 \text{ lb/sq ft}$	$\frac{b}{2} = 20 \text{ ft}$	
$\rho = 0.002378 \text{ slugs/cu ft}$		
$i_A = 0.064$	$\mu_2 = 21$	
$i_C = 0.140$		
$y_v = -0.19$		
$l_v = -0.03$	$l_p = -0.415$	$l_r = +0.24C_L$
$n_v = +0.053$	$n_p = -0.05C_L$	$n_r = -0.044$
$l_\xi = -0.18$		
$n_\xi = +0.02$	$n_\zeta = -0.074$	

The value of  $n_r$  is derived from flight tests, the wind tunnel value is much higher ( $n_r = -0.13$ ). The low value of  $n_r$  was chosen as it gives the worst stability conditions.

<i>Meteor flying at 600 m.p.h. at sea level</i>	<i>Meteor flying at 110 m.p.h. at sea level, with flaps and undercarriage down</i>
---	--

U <sub>e</sub> ft/sec	880	160
$C_L$	0.034	1.0
$\hat{t}$	0.46	2.53
$k$	0.017	0.50
$\bar{y}_v$	0.19	0.19
$l_1$	6.48	6.48
$l_2$	0.13	3.75
$n_1$	0.012	0.357
$n_2$	0.313	0.313
$\mathcal{L}$	9.84	9.84
$\mathcal{N}$	7.95	7.95
$\mathcal{L}_\xi$	56.0	56.0
$\mathcal{N}_\xi$	3.0	3.0
$\mathcal{N}_\zeta$	11.0	11.0

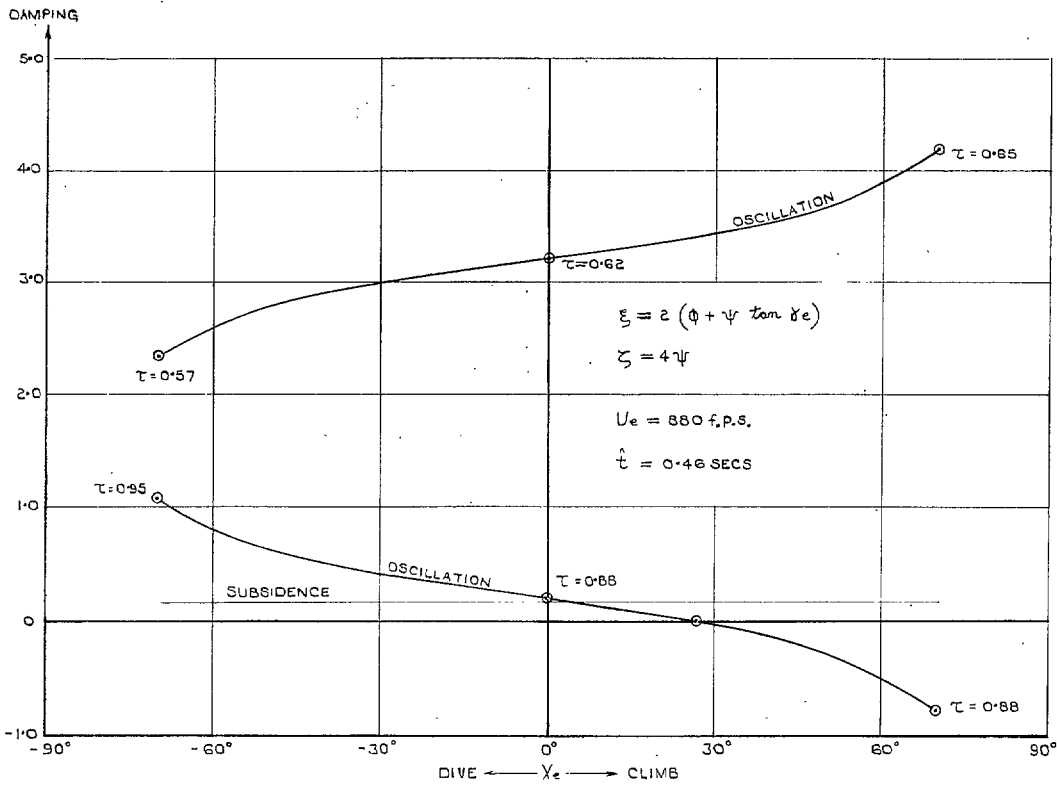


FIG. 1. Lateral stability. Aileron drag uncompensated.

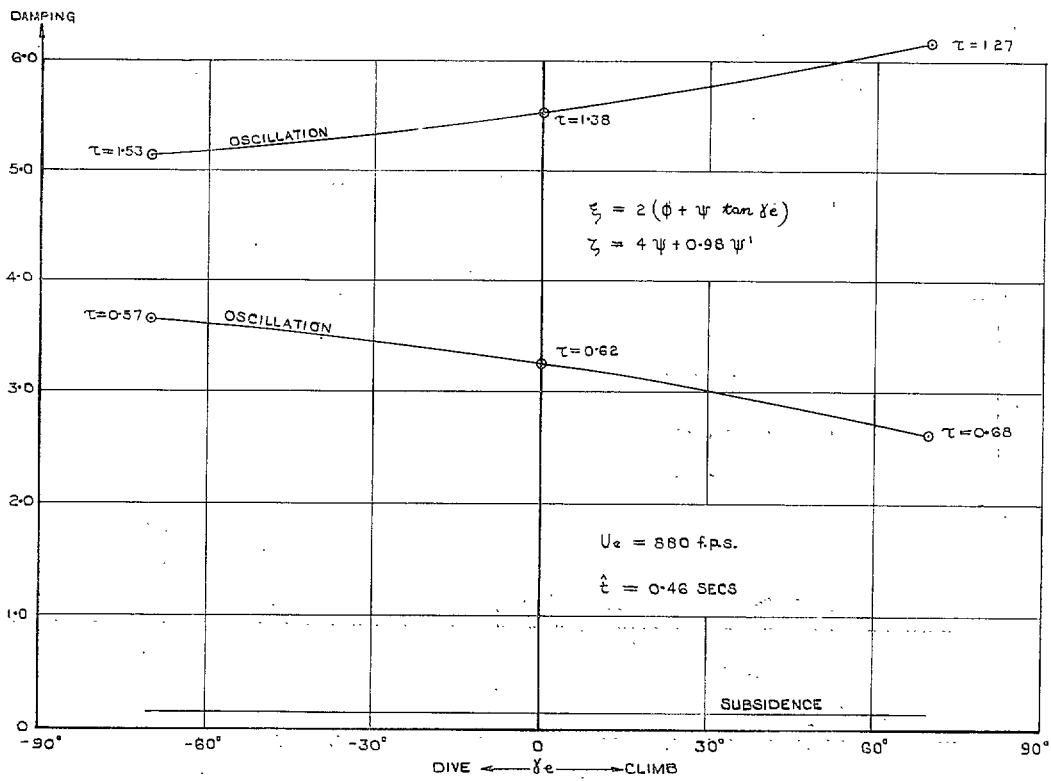


FIG. 2. Lateral stability. Aileron drag uncompensated with addition of rate term.



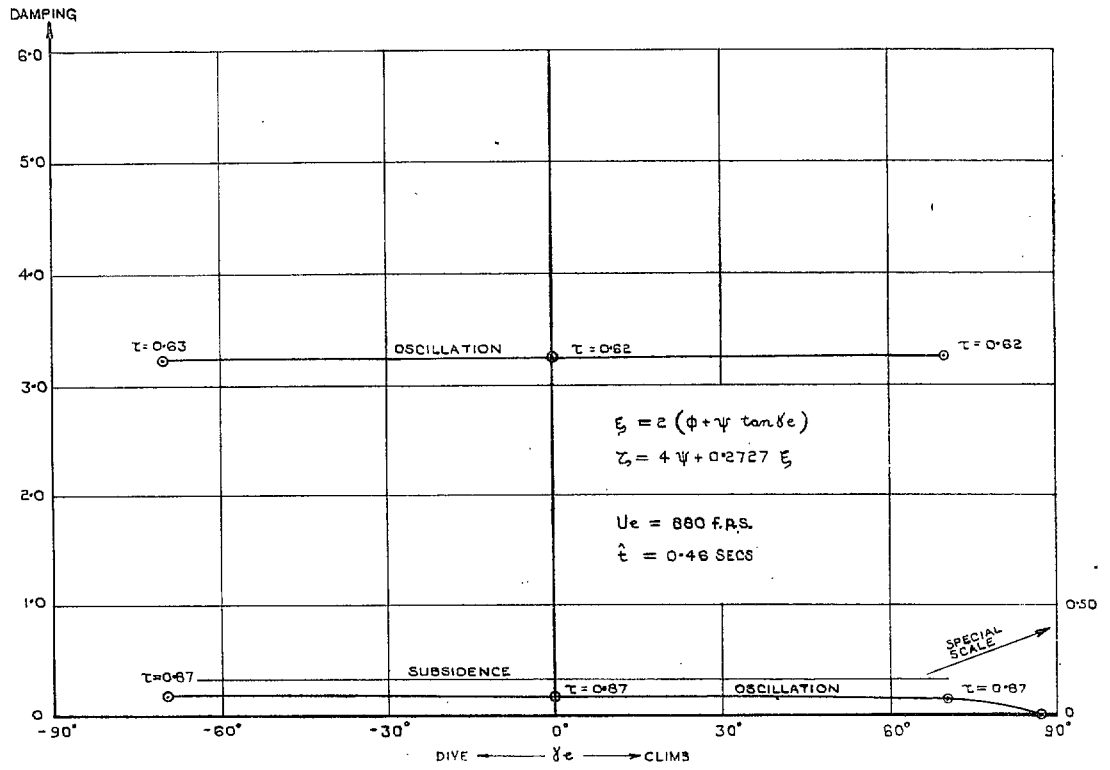


FIG. 3. Lateral stability. Aileron drag compensated.

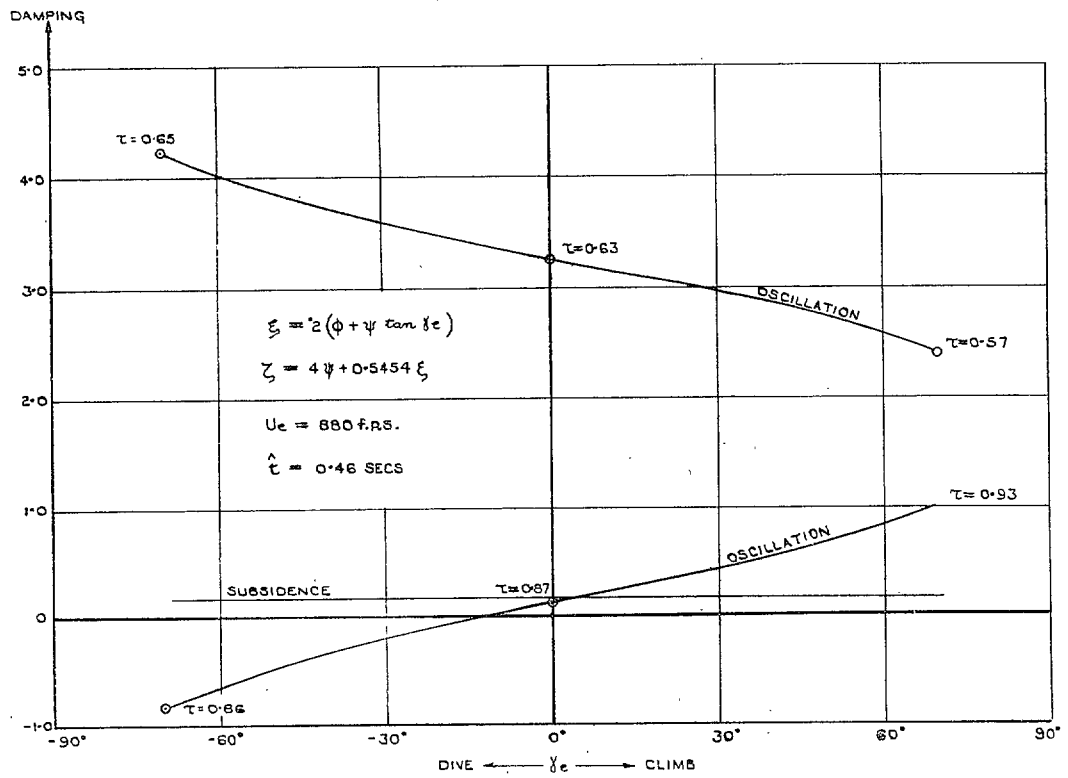


FIG. 4. Lateral stability. Aileron drag over-compensated.

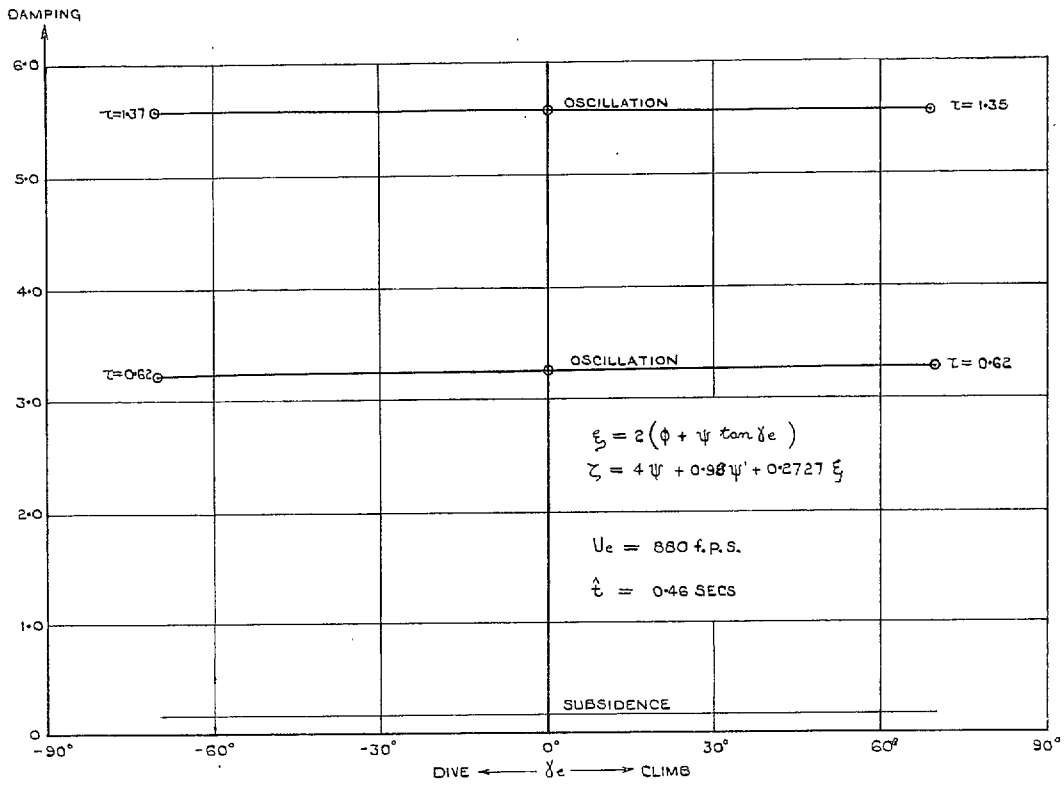


FIG. 5. Lateral stability. Aileron drag compensated with addition of rate term.

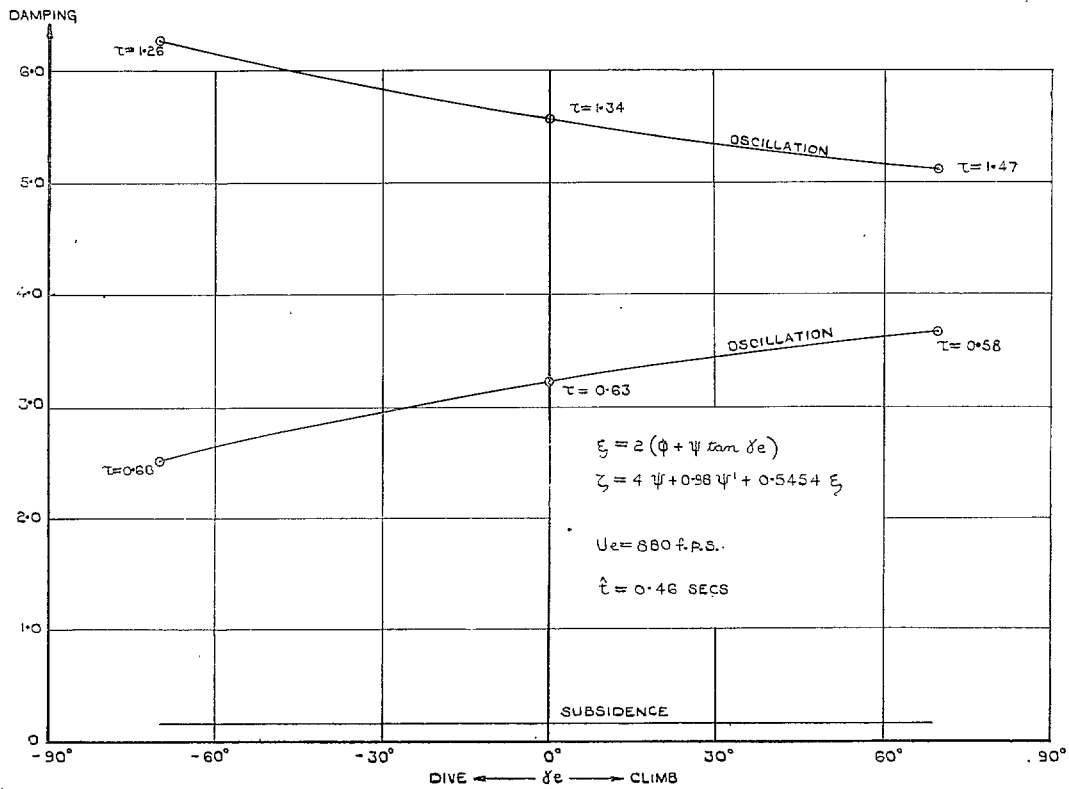


FIG. 6. Lateral stability. Aileron drag over-compensated with addition of rate term.

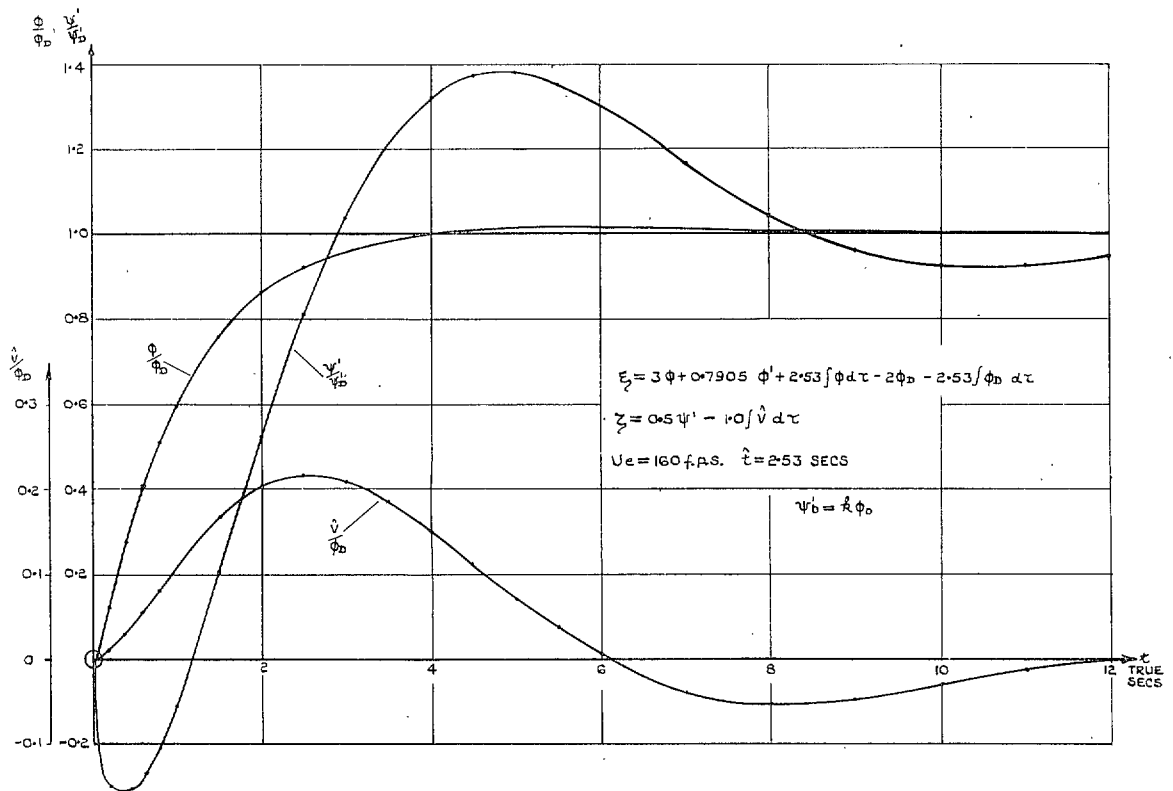


FIG. 7. Turns entry. No compensation for  $\mathcal{N}_\xi$ .

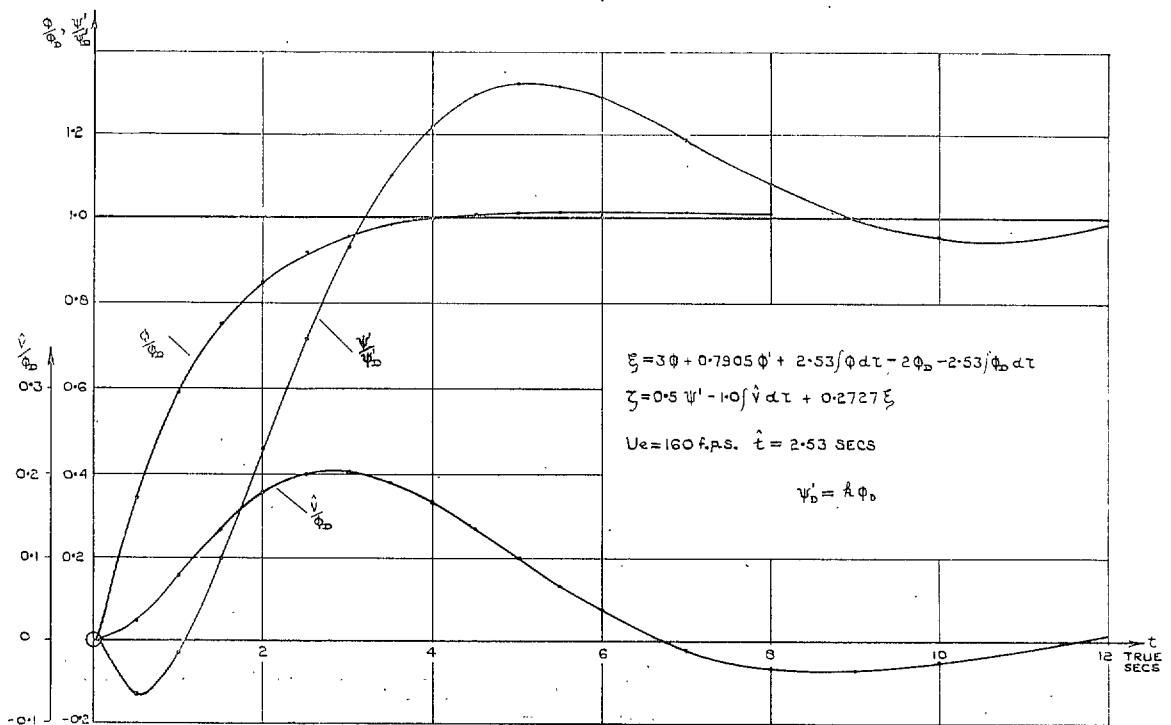


FIG. 8. Turns entry. Exact compensation for  $\mathcal{N}_\xi$ .

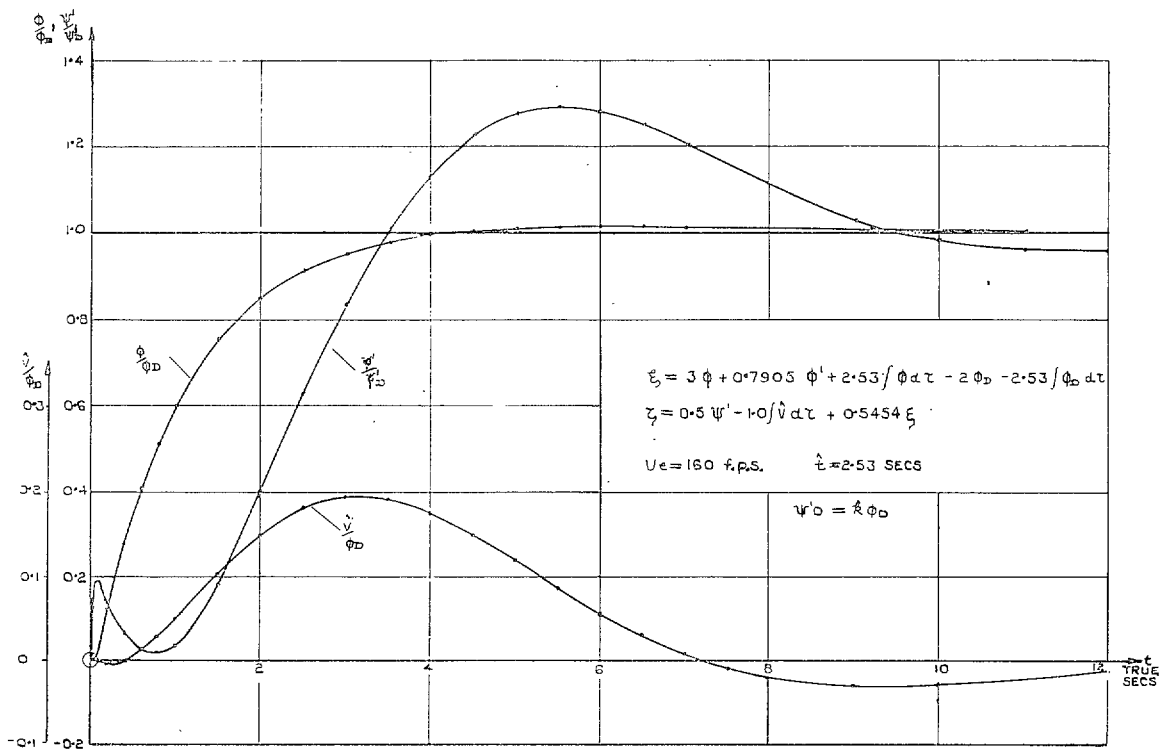


FIG. 9. Turns entry. Over compensation for  $\mathcal{N}_\xi$ .

## Publications of the Aeronautical Research Council

### ANNUAL TECHNICAL REPORTS OF THE AERONAUTICAL RESEARCH COUNCIL (BOUND VOLUMES)—

- 1934-35 Vol. I. Aerodynamics. *Out of print.*  
Vol. II. Seaplanes, Structures, Engines, Materials, etc. 40s. (40s. 8d.)
- 1935-36 Vol. I. Aerodynamics. 30s. (30s. 7d.)  
Vol. II. Structures, Flutter, Engines, Seaplanes, etc. 30s. (30s. 7d.)
- 1936 Vol. I. Aerodynamics General, Performance, Airscrews, Flutter and Spinning. 40s. (40s. 9d.)  
Vol. II. Stability and Control, Structures, Seaplanes, Engines, etc. 50s. (50s. 10d.)
- 1937 Vol. I. Aerodynamics General, Performance, Airscrews, Flutter and Spinning. 40s. (40s. 10d.)  
Vol. II. Stability and Control, Structures, Seaplanes, Engines, etc. 60s. (61s.)
- 1938 Vol. I. Aerodynamics General, Performance, Airscrews. 50s. (51s.)  
Vol. II. Stability and Control, Flutter, Structures, Seaplanes, Wind Tunnels, Materials. 30s. (30s. 9d.)
- 1939 Vol. I. Aerodynamics General, Performance, Airscrews, Engines. 50s. (50s. 11d.)  
Vol. II. Stability and Control, Flutter and Vibration, Instruments, Structures, Seaplanes, etc. 63s. (64s. 2d.)
- 1940 Aero and Hydrodynamics, Aerofoils, Airscrews, Engines, Flutter, Icing, Stability and Control, Structures, and a miscellaneous section. 50s. (51s.)

*Certain other reports proper to the 1940 volume will subsequently be included in a separate volume.*

### ANNUAL REPORTS OF THE AERONAUTICAL RESEARCH COUNCIL—

1933-34	1s. 6d. (1s. 8d.)
1934-35	1s. 6d. (1s. 8d.)
April 1, 1935 to December 31, 1936	4s. (4s. 4d.)
1937	2s. (2s. 2d.)
1938	1s. 6d. (1s. 8d.)
1939-48	3s. (3s. 2d.)

### INDEX TO ALL REPORTS AND MEMORANDA PUBLISHED IN THE ANNUAL TECHNICAL REPORTS, AND SEPARATELY—

April, 1950 R. & M. No. 2600. 2s. 6d. (2s. 7½d.)

### INDEXES TO THE TECHNICAL REPORTS OF THE AERONAUTICAL RESEARCH COUNCIL—

December 1, 1936 — June 30, 1939.	R. & M. No. 1850.	1s. 3d. (1s. 4½d.)
July 1, 1939 — June 30, 1945.	R. & M. No. 1950.	1s. (1s. 1½d.)
July 1, 1945 — June 30, 1946.	R. & M. No. 2050.	1s. (1s. 1½d.)
July 1, 1946 — December 31, 1946.	R. & M. No. 2150.	1s. 3d. (1s. 4½d.)
January 1, 1947 — June 30, 1947.	R. & M. No. 2250.	1s. 3d. (1s. 4½d.)

*Prices in brackets include postage.*

Obtainable from

### HER MAJESTY'S STATIONERY OFFICE

York House, Kingsway, LONDON, W.C.2    423 Oxford Street, LONDON, W.1  
P.O. Box 569, LONDON, S.E.1  
13a Castle Street, EDINBURGH, 2    1 St. Andrew's Crescent, CARDIFF  
39 King Street, MANCHESTER, 2    Tower Lane, BRISTOL 1  
2 Edmund Street, BIRMINGHAM, 3    80 Chichester Street, BELFAST

or through any bookseller.